EXTREME HYDRODYNAMIC FORCES OVER A FLOATING FOUNDATION GENERATED BY LOW SEA STATE: A CFD-FEA MODELING STUDY CASE.

AUTORES

LAURA VALENTINA GIL MUÑOZ.

Artículo científico presentado como requisito para optar al título de:

INGENIERA CIVIL

Director:

JUAN GABRIEL RUEDA BAYONA

UNIVERSIDAD MILITAR NUEVA GRANADA

FACULTAD DE INGENIERIA

PROGRAMA INGENIERIA CIVIL

BOGOTÁ, 25 DE ABRIL DEL 2021

Ocean Engineering

Extreme hydrodynamic forces over a floating foundation generated by low sea state: a CFD-FEA modeling study case.

--Manuscript Draft--

Manuscript Number:	
Article Type:	Full length article
Keywords:	Offshore; numerical modeling; hydromechanics; TLP; Simulation
Corresponding Author:	Juan Gabriel Rueda-Bayona, Ph.D Universidad Militar Nueva Granada Bogotá, COLOMBIA
First Author:	Juan Gabriel Rueda-Bayona, Ph.D
Order of Authors:	Juan Gabriel Rueda-Bayona, Ph.D
	Laura Gil
Abstract:	The high development of the offshore industry for supporting new marine and renewable energy projects requires a constant improvement of methods for structure designing. Because recent studies warned that maximum environmental loads occur during low sea states and not during extreme sea states as recommend the offshore standards (e.g RP 2AWSD-2014), this study used measured wave and current data for validation. The Colombian Caribbean coast was selected as the study area, and in situ ADCP data combined with Reanalysis and numerical data was used for identifying proper sea states for the analysis. Then, 2 low and 1 extreme sea states were selected and their associated current profiles were extracted, for providing input data for CFD-FEA simulations and assessing the effect of the hydrodynamic forces over an offshore structure. The results showed that the current profiles during low sea states generated the maximum structural responses, what evidenced that low wave heights, combined with low wind speeds during Ebb tide, produced the maximum hydrodynamic forces.
Suggested Reviewers:	Andrés Guzman, PhD Professor, Universidad del Norte faguzman@uninorte.edu.co He is expert in offshore engineering in the study area
	Emilio Bastidas, PhD Professor, Nantes University: Universite de Nantes emilio.bastidas@univ-nantes.fr He is expert in marine structures
	Jose Horrillo, PhD Researcher, Swansea University j.m.horrillo-caraballo@swansea.ac.uk He is expert in oceanography en renewable energies

Bogotá, January 24th, 2021

Dr.
Atilla Incecik
Editor in Chief
Ocean Engineering

Ref.:
Extreme hydrodynamic forces over a floating foundation generated by low sea state: a CFD-FEA modeling study case.
Dear Editors.

We are glad to present to your Journal the enclosed paper titled “Extreme hydrodynamic forces over a floating foundation generated by low sea state: a CFD-FEA modeling study case..” This study was funded by the project INV-ING 3196. We hope you and your colleagues find it interesting.

Please do not hesitate in contacting me if you have any further comments.

Sincerely yours,

Juan Gabriel Rueda-Bayona, PhD
Professor
Universidad Militar Nueva Granada
juan.rueda@unimilitar.edu.co
www.umng.edu.co

HIGHLIGHTS

Recent studies warned that maximum environmental loads occurred during low sea states and not during extreme sea states as recommend the offshore standards

In situ ADCP data combined with Reanalysis and numerical data allowed identifying low and extreme sea states and maximum strcutural responses.

This research confirmed that low sea states may generate the maximum hydrodynamic forces over an offshore structure.

Declaration of interests

☒ The authors declare that they have no known competing financial interests or personal relationships that could have appeared to influence the work reported in this paper.

☐The authors declare the following financial interests/personal relationships which may be considered as potential competing interests:

CRediT author statement

Juan Gabriel Rueda-Bayona, Ph.D: Writing - Original Draft, Conceptualization, Methodology, Validation, Formal analysis

Laura Gil: Software, Writing - Original Draft.

Extreme hydrodynamic forces over a floating foundation generated by low sea state: a CFD-FEA modeling study case.

Juan Gabriel Rueda-Bayona[a], Laura Gil [b]

a. Universidad Militar Nueva Granada. Engineering Faculty. Civil Engineering. Water and Energy (AyE) Research Group. Bogotá: Carrera 11 No.101- 80. ORCID: https://orcid.org/0000-0003-3806-2058.Email: juan.rueda@unimilitar.edu.co, ruedabayona@gmail.com.

b. Universidad Militar Nueva Granada. Engineering Faculty. Civil Engineering. Water and Energy (AyE) Research Group. Bogotá: Carrera 11 No.101- 80. ORCID: https://orcid.org/0000-0002-7418-8574 .Email: u1102838@unimilitar.edu.co, lauravalentinagilm99@gmail.com.

Abstract.

The high development of the offshore industry for supporting new marine and renewable energy projects requires a constant improvement of methods for structure designing. Because recent studies warned that maximum environmental loads occur during low sea states and not during extreme sea states as recommend the offshore standards (e.g RP 2AWSD-2014), this study used measured wave and current data for validation. The Colombian Caribbean coast was selected as the study area, and in situ ADCP data combined with Reanalysis and numerical data was used for identifying proper sea states for the analysis. Then, 2 low and 1 extreme sea states were selected and their associated current profiles were extracted, for providing input data for CFD-FEA simulations and assessing the effect of the hydrodynamic forces over an offshore structure. The results showed that the current profiles during low sea states generated the maximum structural responses, what evidenced that low wave heights, combined with low wind speeds during Ebb tide, produced the maximum hydrodynamic forces.

Keywords: Offshore, numerical modeling, hydromechanics, TLP, Simulation

Introduction.

The increasing interest for non-conventional renewable energies worldwide motivated several countries to develop technologies such as offshore wind turbines (Rueda-Bayona et al., 2019a). These offshore projects require rigorous engineering designing because of the complex fluid-structure interactions (environmental loads) that face the wind turbine foundations, in this sense, subjective designs may put at risk their stability that would generate environmental and operational problems. The traditional designing guidelines for marine structures recommend characterizing the wave climate to identify the designing load from the extreme sea states (API, 2011, 2007b, 2007a, 2001; British Standard, 2015, 2008; Det Norske Veritas AS, 2014; International Electrotechnical Commission, 2009; International Organization for Standardization, 2015, 2013; NORSOK, 2017).

The increasing interest of developing offshore wind turbines is evidenced in recent studies. Pham and Shin (2019) (Dai et al., 2018) (Sarkar et al., 2020) (Chen et al., 2018) (Manikandan and Saha, 2019). Kim and Shin, (2020) validated the numerical modeling of a 1:40 scale model under different environmental loads in a wave flume, and (Li et al., 2018), studied the transient responses of a SPAR-type turbine when one of the mooring lines suddenly fractures under extreme sea states. In Australia (Tian et al., 2018) studied the optimization of offshore wind turbine anchors considering specific wave parameters for the environmental loads. (Chuang

et al., 2020) investigated how the mean drift force of the wave and the slow drift load of the platform influenced the movements of a platform, and concluded that the average drift force and slow drift force moved the structure away along the direction of wave propagation.

The complex fluid-structure interactions of offshore foundations have been studied through numerical approaches (physical modeling), to understand how the hydrodynamic forces affect the dynamic and mechanical properties of diverse marine structures. (Bruinsma et al., 2018) analyzed the vertical movements of a moored floating structure through numerical modeling, and compared successfully the complex fluid-structure interactions against measured experimental results. Ishihara and Zhang (2019) developed a non-linear simulation tool coupled to the Morrison equation to determine the dynamic response of a floating structure and concluded that the quasi-static model successfully reproduced the first three main displacements, and (Cheng et al., 2019) performed CFD modeling of a floating offshore wind turbine through the OpenFOAM to analyze the fluid-structure interactions under several sea state conditions. (Yue et al., 2020) analyzed the hydromechanics of a Spar floating platform through the numerical model ANSYS-AQWA, and (Barooni et al., 2018) and (Sant et al., 2018) used the same software to analyze the hydromechanics of and offshore wind turbine under different environmental loads.

However, Rueda-Bayona et al. (2019b) revised these guidelines and warned that extreme hydrodynamic forces did not occur during extreme sea states (high surface waves), but these extreme forces appeared during low sea states with wave height less than 1 m. The authors recommended inspecting low sea states for identifying extreme hydrodynamic forces when the offshore foundation is under inertia regime (Chakrabarti, 2005), which is the most common regime for offshore wind turbine: water depth > 30 m, wave heights > 1 m, and wave period higher than 4 s. Also, the literature review performed by Rueda-Bayona et al. (2019b) showed that several studies considered the standard guidelines for analyzing the structural dynamics of offshore structures, then, these researches omitted that during low sea-states a non-uniform current profile may generate more hydrodynamic forces than can produce high waves during extreme sea-states such as hurricanes or cold fronts.

The revised literature showed that offshore designing may be excluding extreme hydrodynamic forces during low sea-states because of the standards recommendation of selecting environmental design loads from extreme sea-states. In this sense, this study used measured current profiles during low and extreme sea-states to verify if maximum hydrodynamic forces may occur under low sea-states as pointed Rueda-Bayona et al. (2019b) through modelled current profiles. Then, the measured current profiles were used as environmental loads to analyze their effect over the nearfield hydrodynamics and the mechanical properties of a Tension-leg foundation. This study is a contribution to highlight the relevance of identifying extreme hydrodynamic forces higher that could be seen during extreme wave states recommended by the designing standard. The CFD modelling with measured data of this study provides more evidence that low-sea states may generate critical structural responses because current profiles generate more effect than extreme waves if the offshore structure is in an inertia regime.

Methodology.

The strategy for analyzing the effect of extreme current profiles generated during low sea states comprises three main steps: 1- Identification of the sea states and profile selection, 2- hydrodynamic modeling, 3- Structural simulations.

After defining the study area, *in situ* ocean data was necessary to identify low and extreme sea states for the current profile selection. The study case was performed in the Colombian Caribbean coast where the in situ

data was retrieved from the study of Rueda-Bayona (2017) and Rueda-Bayona et al., (2020), who used measured data from an Acoustic Doppler Current Profiler (ADCP) located in 11.038° N 74.943° W (Fig. 1). The ADCP measured at 8 m water-depth and recorded wave and current data from June 3rd to December 11th of 2015 with 10 minutes of interval.

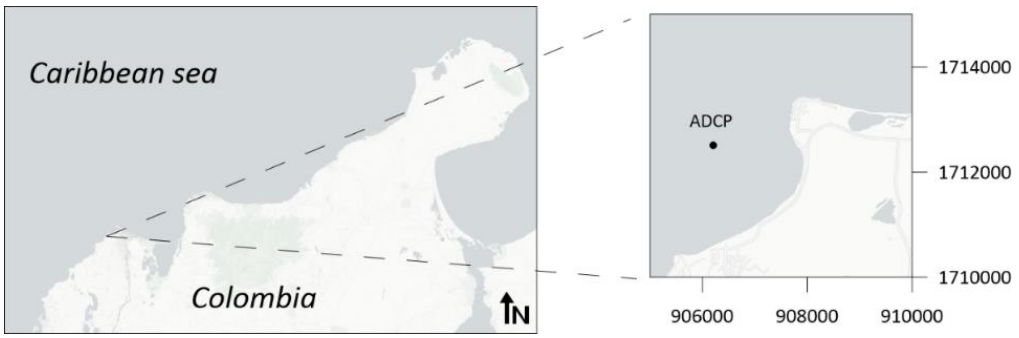

Fig. 1. Study area and location of the in situ current profiles measured by ADCP. Coordinates in Magna Sirgas (Bogotá zone).

The surface wind data was downloaded and processed from the NARR-NOAA database (NOAA, 2016) which has a 3-hourly time interval of frequency. The water level data was generated through the hydrodynamic Delft3D model, which was previously implemented and calibrated by (Rueda-Bayona et al., 2020e).

The characteristics of the control volume, the foundation location, and the selected layers (planes) for the CFD analysis are depicted in Fig. 2a. The TLP foundation(Fig. 2b) is perfectly fixed into the seafloor to analyze the effect of currents over the near hydrodynamic field of a non-mobile solid, and how the hydrodynamic forces affect the main mechanical properties of the foundation such as the Von Misses stress.

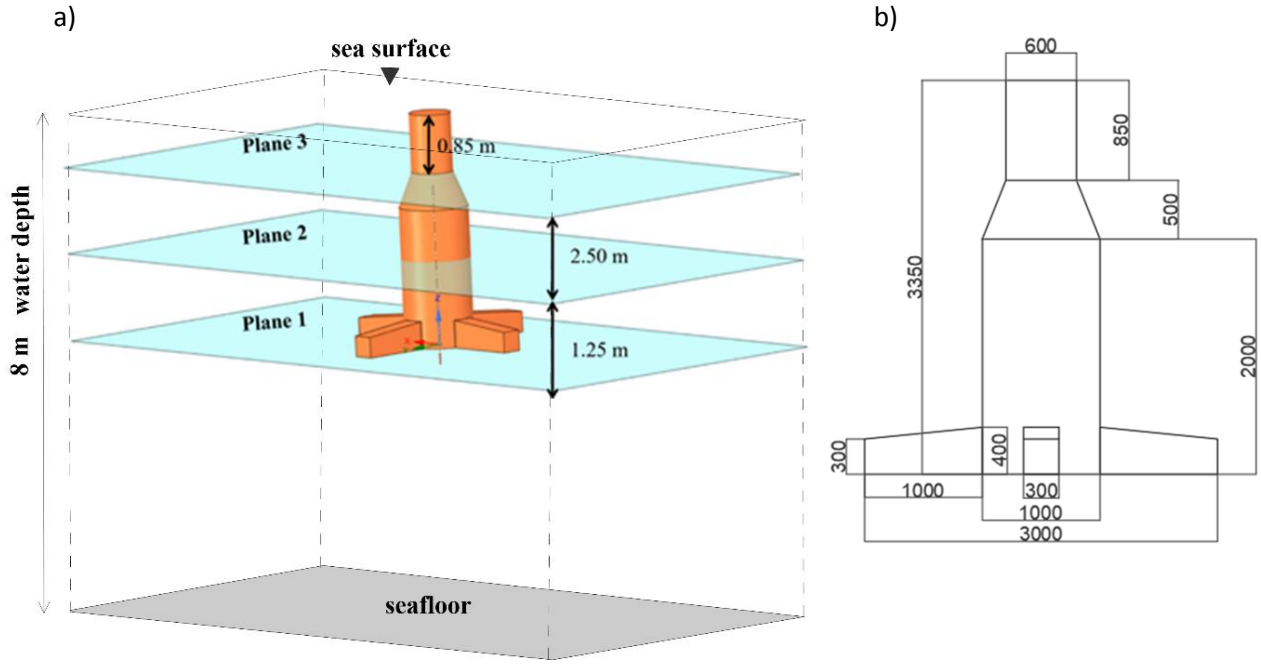

Fig. 2. a) numerical control volume and plane views of TLP foundation for the CFD modeling, b) main dimensions of TLP foundation; units in millimeters.

The CFD (Computational Fluid Dynamics) and FEA (Finite Element Analysis) were performed through the ANSYS software V.2019 R2 (www.ansys.com), which is a multiphysics numerical model able to simulate complex fluid-structure interactions and other physical problems. The numerical strategy to simulate the effects of the extreme current profiles (Fig. 5) over the TLP foundation (Fig. 2) is shown in the Fig. 3, where the CFD analysis will be done by the Fluent model (Fluid Flow) known as Ansys-Fluent, and the FEA through the structural model (Static structural) known as Ansys-Mechanical. The Ansys-Fluent solves the Reynold Averaged Navier-Stokes (RANS) equations for computing properties of the hydrodynamic field (velocities, pressures, forces, and turbulent parameters), and the Ansys-Mechanical uses the hydrodynamic data generated by Ansys-Fluent to calculate deformations and mechanical parameters of the solid body.

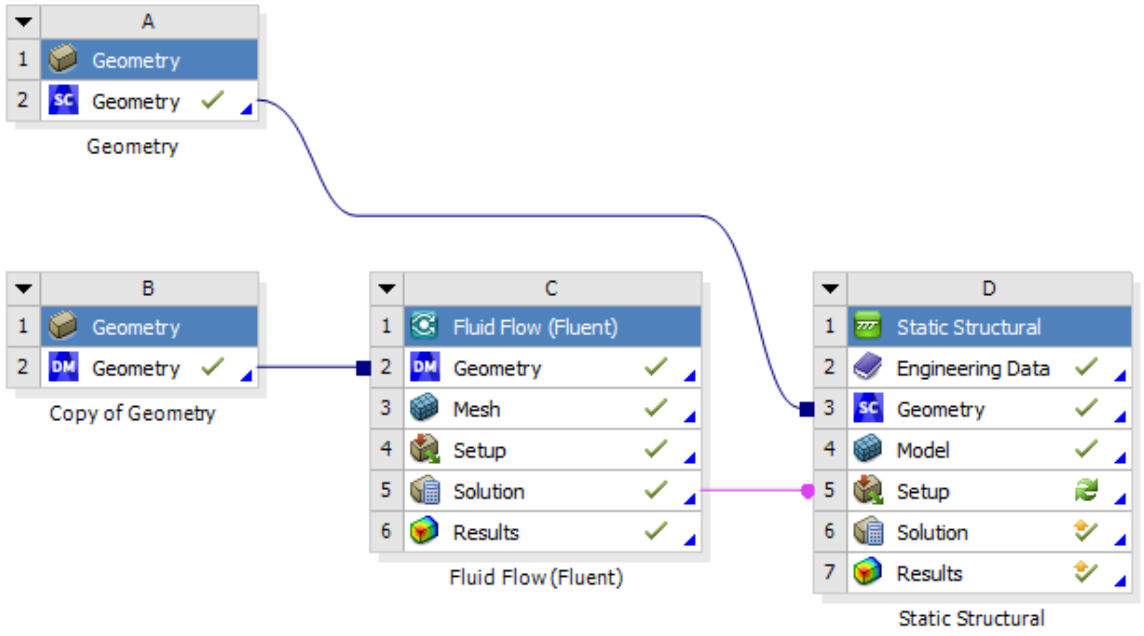

Fig. 3. Structure of the numerical approach and data pathlines in the ANSYS Workbench.

The properties and boundary conditions of the CFD model are seen in Table 1, such as the fluid control volume characteristics and the applied numerical methods. The parameters and values of the ANSYS-Fluent model were tuned considering the convergence of the numerical solution and the expected behavior of magnitude and shape of the hydrodynamic field perturbed by a monopile (Journée and Massie, 2002; Sarpkaya, 1993) and by the current field nearby to the study area (Juan Gabriel Rueda-Bayona, 2017; Rueda-Bayona et al., 2020c, 2020a, 2019b). The mechanical properties of the TLP foundation such as the Isotropic Elasticity derived from Young's Modulus and Poisson's Ratio are listed in Table 2.

Table 1. Fluid properties, boundary conditions, and numerical approach of the CFD model (ANSYS-Fluent).

Parameter	**value**
seawater density (kg/m^3)	1020
kinematic viscosity	0.0002
solver	pressure based
velocity formulation	absolute
time	steady
z gravity	-9.81
steel density (kg/m^3) - solid	7850
boundary conditions	upstream

velocity specification method	magnitude, normal to boundary
reference frame	absolute
turbulence - method	Intensity and Viscosity ratio
Turbulent intensity (%)	5
Turbulent viscosity ratio	10
Solution methods	
Pressure-velocity coupling	Yes
Scheme	coupled
Spatial discretization	
Gradient	Least Squares Cell based
Pressure	Second order
Momentum	Second order Upwind
Turbulent Kinetic Energy	1st order upwind
Specific dissipation rate	1st order upwind
pseudo transient	yes
Pressure	0.5
Momentum	0.5
Density	1
Body forces	1
Turbulent Kinetic Energy	0.75
Specific dissipation rate	0.75
Turbulent viscosity	1

Table 2. Mechanical properties of the TLP foundation for the FEA through ANSYS-Mechanical.

Parameters	**value**
Young's Modulus (Pa)	2.00E+11
Poisson's Ratio	0.3
Bulk Modulus (Pa)	1.67E+11
Shear Modulus (Pa)	7.69E+10
Isotropic Secant Coefficient of Thermal Expansion 1/°C	1.20E-05
Compressive Ultimate Strength (Pa)	0
Compressive Yield Strength (Pa)	2.50E+08
Tensile Ultimate Strength (Pa)	4.60E+08
Tensile Yield Strength (Pa)	2.50E+08

Results and Discussion

The identification of the low and extreme sea states of the study area considered the climate analysis performed by previous studies, which pointed to a low sea state when significant wave heights (Hs) are below 1.28 m and an extreme sea state occurs when Hs is higher than 2.87 m (Rueda-Bayona et al., 2020b, 2020d; Rueda-Bayona and Guzmán, 2020). In this sense, the evolution of significant wave heights (Hs) generated from the ADCP data allowed identifying 3 sea states (Fig. 4) pointed as run 1, 2, and 3, which 2 of them (run 1 and 3) occurred during low sea conditions, and the third sea state (run 2) showed extreme sea conditions. Considering that winds and water level induce the generation of extreme hydrodynamic forces (Rueda-

(Rueda-Bayona et al., 2019b), the evolution of these parameters were plotted together with the Hs and wave direction (Fig. 4); waves and winds have an oceanographic convention, winds come from and waves go to.

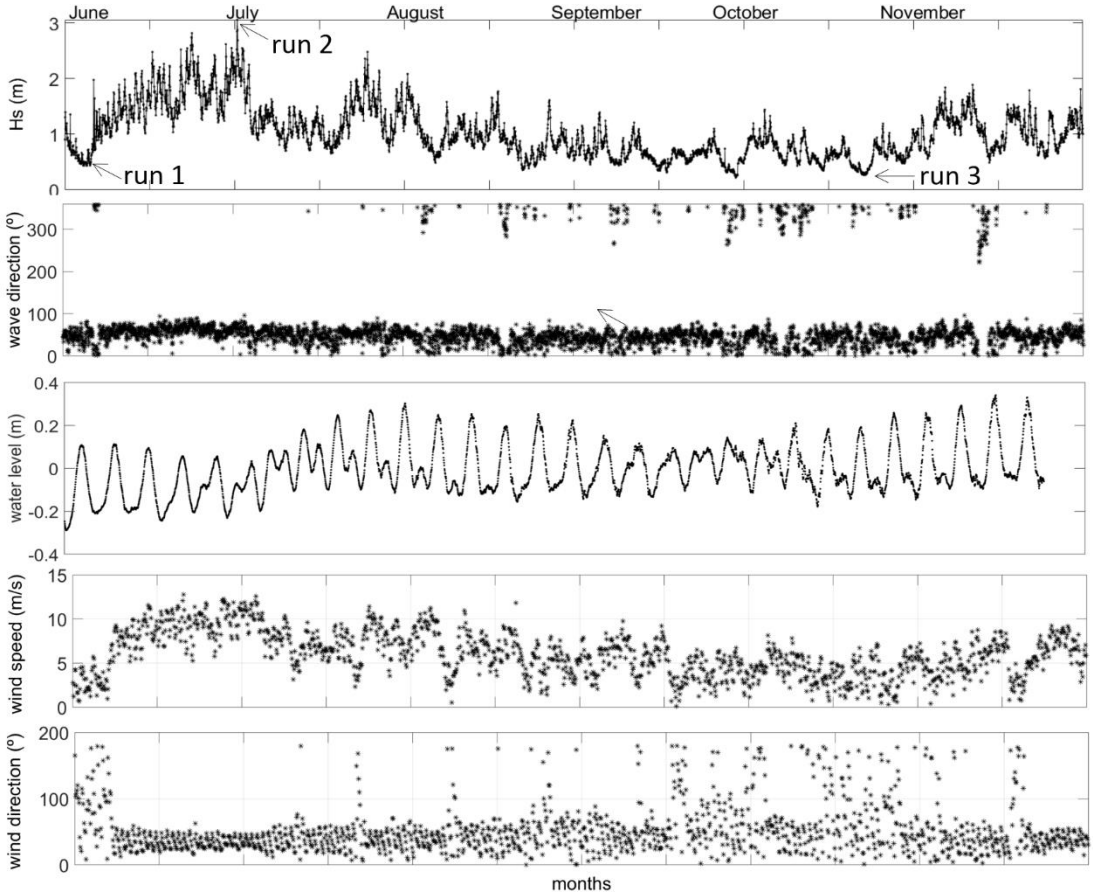

Fig. 4. Oceanographic data from June 3rd to December 12th of 2015. The ADCP wave time series and 10-m wind data of the study area were edited from (Juan Gabriel Rueda-Bayona, 2017).

From the 3 sea states selected 3 current profiles were selected, each of them associated to an extreme and low sea state (Table 3). The measured current profiles had 0.4 m of cell size with 0.4 m of blanking, what represented 20 measurement points alongside the 8 m of water column (Fig. 5).

Table 3. Oceanographic parameters of the 3 selected ADCP current profiles.

	Date – time	**Hs (m)**	**Tp (s)**	**Wave direction (°)**	**Wind speed (m/s)**	**Wind direction (°)**	**sea-state**	**Tide condition**	**Run**
June	3/06/2015 -10:00	0.44	7.76	56	2.40	50	low	Ebb	1
July	4/07/2015 - 2:00	3.06	10.78	60	11	33	extreme	Ebb	2
October	15/10/2015 -3:00	0.3413	6.92	30	5.82	31	low	Ebb	3

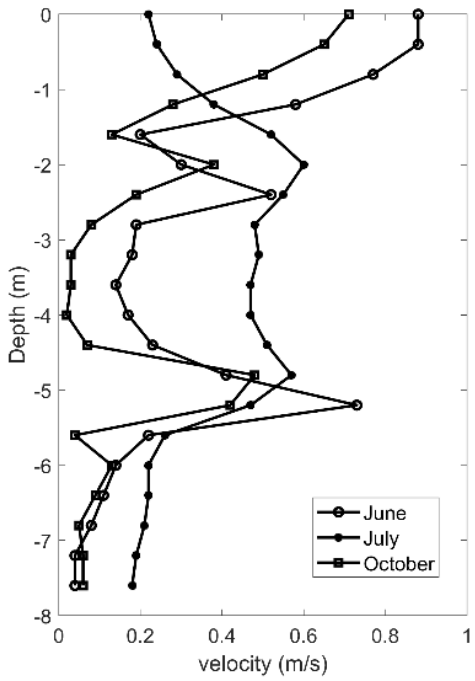

Fig. 5. ADCP Current velocity profiles and b) Geometry of the TLP foundation.

After the identification of low and extreme sea states and the current profile selection, the CFD simulations were performed. Then, the hydrodynamic results during the fluid structure interactions between the current profiles and the TLP foundation are shown in Fig. 6. The CFD results evidenced that the maximum current velocity occurred during the low sea states of June and October (Table 3), then, the maximum hydrodynamic forces were generated during these two sea sates where the Hs did not exceed the 0.5 m (low sea state). The maximum current velocities were observed in June (Fig. 6 a, d, g) with values about 1 m/s nearby to the TLP legs, followed by the results of October which not exceeded the 0.9 m/s in the upper planes of the hydrodynamic fields (Fig. 6 f, i).

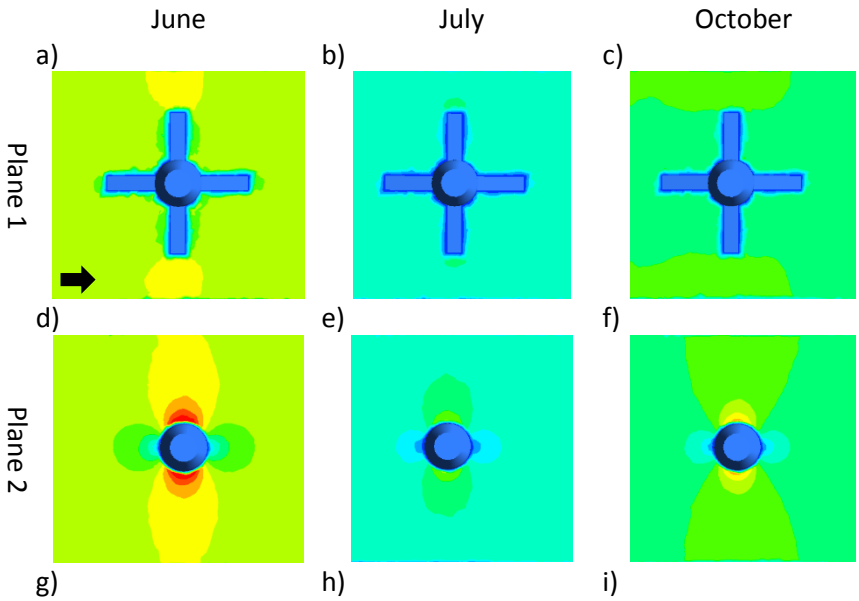

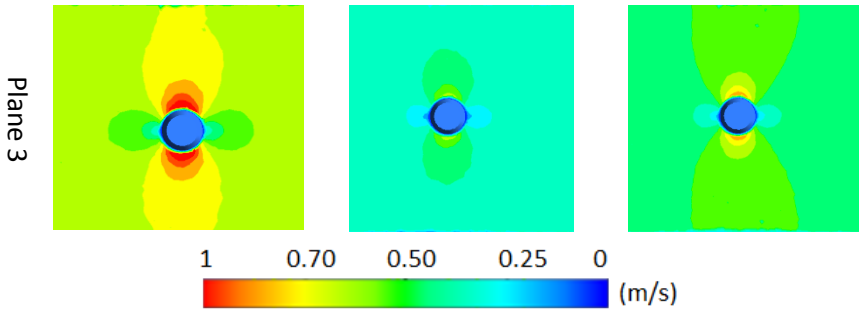

Fig. 6. Velocity contours generated by the current velocity profiles during extreme and low sea states occurred in June, July, and October of the 2015 year; the black arrow represents the upstream flow.

The results of July showed that current velocities were not higher than 0.7 m/s (Fig. 6 b, e, h), evidencing that maximum velocities did not occur during the high wave heights of July (Table 3). Then, the derived contour velocities from the CFD results (Fig. 6) pointed that low sea states are associated with extreme current profiles in the study area similar to the statements of Juan Gabriel Rueda-Bayona (2017). The streamlines generated by the CFD modeling showed the hydrodynamic behavior during the effect of current profiles (Fig. 7), which showed the aforementioned maximum velocities during June and October (low sea states) (Fig. 6). The subcritical regime of Reynolds number (Re=2500), the Keulegan-Carpenter number (KC = 9), the hydrodynamic streamlines and a previous inspection of vector field did not suggest the generation of vortex around the TLP foundation.

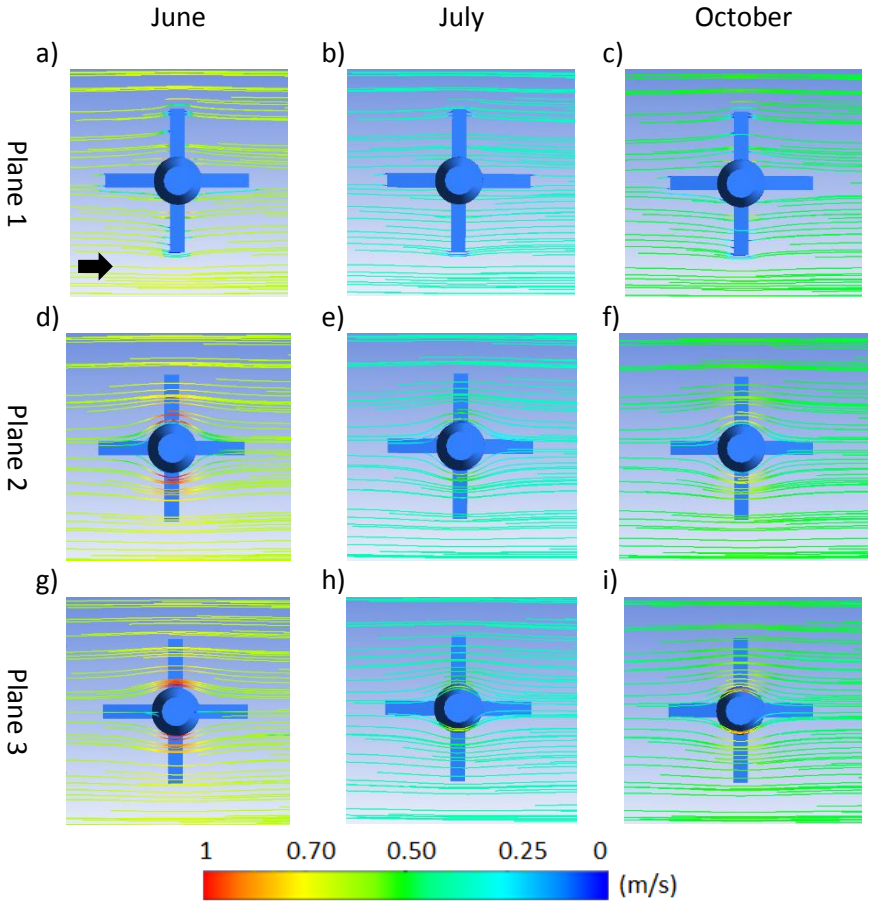

Fig. 7. Streamlines generated by the current velocity profiles during extreme and low sea states occurred in June, July, and October of the 2015 year; the black arrow represents the upstream flow.

In order to identify the effect of the measured current profiles over the TLP foundation during the low and extreme sea states of the study area (Table 3), the hydrodynamic results of the Ansys-Fluent model were transferred to the Ansys-Mechanical model (Fig. 3) in terms of hydrodynamic loads. The FEA performed by Mechanical-Ansys pointed that the maximum stress occurred during June with a value of 8.3969 x 10^5 Pa.(Fig. 8 a, d), where the maximum stresses appeared at the top of the cylinder section (600 m of diameter) (Fig. 2b) and at the 4 TLP legs; the minimum Von Miss stress was 0.1868 Pa occurred in October (Fig. 8 c, f, i).

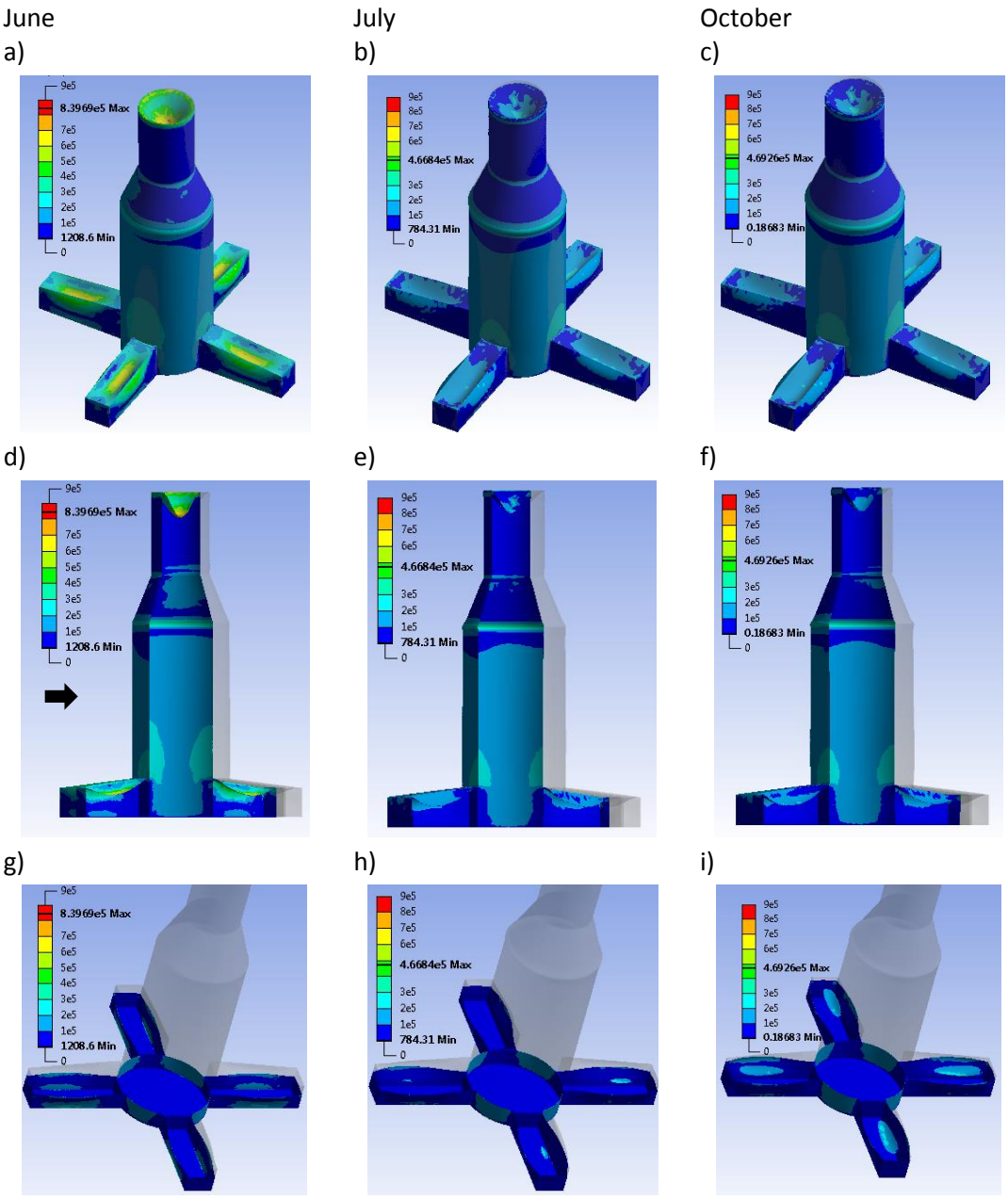

Fig. 8. Von Mises stress (Pa) generated by the current velocity profiles during extreme and low sea states occurred in June, July, and October of the 2015 year; the black arrow represents the upstream flow.

The maximum stress of the TLP foundation generated by the current profiles of June, July, and October showed similar values (0.84 MPa) to the reported by (Rueda-Bayona et al., 2019b) (1.95 MPa), who modelled Von Misses stress of an offshore monopile under similar oceanographic conditions, used the same steel for the foundation located in the same region (Colombian Caribbean coast). As was stated by Rueda-Bayona et al., (2019b) in their study, the maximum hydrodynamic force of this study occurred during a low sea state with a wave height less than 0.7 m and a wind speed less than 4 m/s.

The isobaths and coastline orientation also were similar to the study of Rueda-Bayona et al., (2019b), as well as the wind characteristics, but wave directions of this study were different because the waves propagated to the east due to the wave-refraction generated by the water depth reduction nearby the shore. Because the waves of that study propagated to the south-east and the flood tide was just starting, these forcers eased the water flux development which generated the maximum hydrodynamic forces. In this study, the ebb tide was at the half period where the maximum accelerations occurred. As a result, the maximum currents of the ebb tide combined with a low sea state and winds blowing from the east (30°-50°) eased the increment of current velocities as seen in the profiles of June and October (run 1 and 3) (Fig. 5). The current profile of July showed the lowest magnitudes because the potential energy of its high waves reduced the kinetic energy at the surface. Considering that this study area is nearby to the surface river plume of Magdalena River (Alvarez-Silva and Osorio, 2014; Restrepo and López, 2008), the generated currents close to shore which flow to the southeast, combined with the ebb tide, winds from the northeast and reduced wave heights, generated maximum hydrodynamic forces at the study area during low sea state conditions.

Conclusions.

The offshore structure design considers that maximum hydrodynamic forces appear during extreme sea states (highest wave height), in this sense, the standard and guidelines suggest selecting the wave parameters of these extreme events for estimating the environmental loads. Considering that recent studies that utilized numerical modelling reported that maximum hydrodynamic forces occurred during low sea states, this study used measured wave and current data for validating if maximum hydrodynamic forces may occur during low sea states.

As a result, 3 sea states were analyzed in the Colombian Caribbean Coast, and their associated current profiles were extracted for the analysis. The current profiles of June, July, and October of the 2015 year were used to perform CFD and FEA simulations of a TLP foundation. The results evidenced that maximum Von Misses stress appeared in June during a low sea state, and not during July, where the maximum wave heights were 3 m. Then, the results of other studies reporting that low sea states generate higher hydrodynamic forces than extreme sea states were confirmed by this study.

This study validates the findings of the recent studies which suggested that maximum hydrodynamic forces occur during low sea states, and their increment depends on the wind-wave-tides interactions and by the geomorphological and bathymetry characteristics. Finally, this research evidenced that Ebb tides during a low sea state ($H_s < 0.5$ m), wind speed less than 4 m/s blowing from the northeast, generate maximum hydrodynamic forces at the study area. As future research it is recommended to analyzing low sea states in different regions with higher latitudes, to confirm the applicabilty of selecting low sea states for identifiying extreme hydrodynamic forces.

Acknowledgments

The authors wish to thank the Universidad Militar Nueva Granada for financial support through the research project INV-ING-3196.

References

Alvarez-Silva, O., Osorio, A.F., 2014. Salinity gradient energy potential in Colombia considering site specific constraints. Renew. Energy 74, 737–748. https://doi.org/10.1016/j.renene.2014.08.074

API, 2011. API RP 2FPS: Recommended practice for planning, designing, and constructing floating production systems, 2nd ed.

API, 2007a. API BULL 2INT-DG: Interim Guidance for Design of Offshore Structures for Hurricane Conditions.

API, 2007b. Recommended Practice for Planning , Designing and Constructing Fixed Offshore Platforms — Working Stress Design. Api Recomm. Pract. 24-WSD, 242. https://doi.org/10.1007/s13398-014-0173-7.2

API, 2001. Recommended Practice for Design and Hazards Analysis for Offshore Production Facilities. Api Recomm. Pract. 14J (Rp 14J).

Barooni, M., Ale Ali, N., Ashuri, T., 2018. An open-source comprehensive numerical model for dynamic response and loads analysis of floating offshore wind turbines. Energy 154, 442–454. https://doi.org/10.1016/j.energy.2018.04.163

British Standard, 2015. BS ISO 29400:2015: Ships and marine technology. Offshore wind energy. Port and marine operations.

British Standard, 2008. BS EN ISO 19902:2007+A1:2013: Petroleum and natural gas industries. Fixed steel offshore structures, 1st ed.

Bruinsma, N., Paulsen, B.T., Jacobsen, N.G., 2018. Validation and application of a fully nonlinear numerical wave tank for simulating floating offshore wind turbines. Ocean Eng. 147, 647–658. https://doi.org/10.1016/j.oceaneng.2017.09.054

Chakrabarti, S.K., 2005. Handbook of offshore engineering, 1st ed.

Chen, L., Basu, B., Nielsen, S.R.K., 2018. A coupled finite difference mooring dynamics model for floating offshore wind turbine analysis. Ocean Eng. 162, 304–315. https://doi.org/10.1016/j.oceaneng.2018.05.001

Cheng, P., Huang, Y., Wan, D., 2019. A numerical model for fully coupled aero-hydrodynamic analysis of floating offshore wind turbine. Ocean Eng. 173, 183–196. https://doi.org/10.1016/j.oceaneng.2018.12.021

Chuang, Z., Liu, S., Lu, Y., 2020. Influence of second order wave excitation loads on coupled response of an offshore floating wind turbine. Int. J. Nav. Archit. Ocean Eng. 1–9. https://doi.org/10.1016/j.ijnaoe.2020.01.003

Dai, J., Hu, W., Yang, X., Yang, S., 2018. Modeling and investigation of load and motion characteristics of offshore floating wind turbines. Ocean Eng. 159, 187–200. https://doi.org/10.1016/j.oceaneng.2018.04.003

Det Norske Veritas AS, 2014. DNV-OS-J101 Design of Offshore Wind Turbine Structures.

International Electrotechnical Commission, 2009. IEC 61400-3 Ed. 1.0 b:2009: Wind turbines - Part 3: Design requirements for offshore wind turbines.

International Organization for Standardization, 2015. ISO 19901-1:2015: Petroleum and natural gas industries - Specific requirements for offshore structures - Part 1: Metocean design and operating considerations.

International Organization for Standardization, 2013. ISO 19900:2013: Petroleum and natural gas industries - General requirements for offshore structures. International Organization for Standardization.

Ishihara, T., Zhang, S., 2019. Prediction of dynamic response of semi-submersible floating offshore wind turbine using augmented Morison's equation with frequency dependent hydrodynamic coefficients. Renew. Energy 131, 1186–1207. https://doi.org/10.1016/j.renene.2018.08.042

Journée, J.M.J., Massie, W.W., 2002. Offshore Hydromechanics, Electrochimica Acta.

Kim, J., Shin, H., 2020. Validation of a 750 kW semi-submersible floating offshore wind turbine numerical model with model test data, part II: Model-II. Int. J. Nav. Archit. Ocean Eng. 12, 213–225. https://doi.org/10.1016/j.ijnaoe.2019.07.004

Li, Y., Zhu, Q., Liu, L., Tang, Y., 2018. Transient response of a SPAR-type floating offshore wind turbine with fractured mooring lines. Renew. Energy 122, 576–588. https://doi.org/10.1016/j.renene.2018.01.067

Manikandan, R., Saha, N., 2019. Dynamic modelling and non-linear control of TLP supported offshore wind turbine under environmental loads. Mar. Struct. 64, 263–294. https://doi.org/10.1016/j.marstruc.2018.10.014

NOAA, 2016. NCEP North American Regional Reanalysis: NARR [WWW Document].

NORSOK, 2017. NORSOK N-003:2017: Actions and actions effects, 3rd ed. Norway.

Pham, T.D., Shin, H., 2019. Validation of a 750 kW semi-submersible floating offshore wind turbine numerical model with model test data, part I: Model-I. https://doi.org/10.1016/j.ijnaoe.2019.04.005

Restrepo, J.D., López, S.A., 2008. Morphodynamics of the Pacific and Caribbean deltas of Colombia, South America. J. South Am. Earth Sci. https://doi.org/10.1016/j.jsames.2007.09.002

Rueda-Bayona, J G, 2017. Identificación de la influencia de las variaciones convectivas en la generación de cargas transitorias y su efecto hidromecánico en las estructuras Offshore. Universidad del Norte.

Rueda-Bayona, Juan Gabriel, 2017. Identificación de la influencia de las variaciones convectivas en la generación de cargas transitorias y su efecto hidromecánico en las estructuras Offshore (PhD Thesis). Universidad del Norte, Barranquilla, Colombia.

Rueda-Bayona, J.G., Guzmán, A., 2020. Genetic algorithms to solve the jonswap spectra for offshore structure designing, in: Proceedings of the Annual Offshore Technology Conference. https://doi.org/10.4043/30629-ms

Rueda-Bayona, J.G., Guzmán, A., Cabello Eras, J.J., 2020a. Selection of JONSWAP Spectra Parameters during Water-Depth and Sea-State Transitions. J. Waterw. Port, Coast. Ocean Eng. 6, 14. https://doi.org/10.1061/(ASCE)WW.1943-5460.0000601

Rueda-Bayona, J.G., Guzmán, A., Cabello, J.J., 2020b. Selection of JONSWAP Spectra Parameters for Water-Depth ans Sea-State Transitions. J. Waterw. Port, Coastal, Ocean Eng. https://doi.org/10.1061/(ASCE)WW.1943-5460.0000601

Rueda-Bayona, J.G., Guzmán, A., Eras, J.J.C., Silva-Casarín, R., Bastidas-Arteaga, E., Horrillo-Caraballo, J., 2019a. Renewables energies in Colombia and the opportunity for the offshore wind technology. J. Clean. Prod. 220, 529–543. https://doi.org/10.1016/j.jclepro.2019.02.174

Rueda-Bayona, J.G., Guzmán, A., Silva, R., 2020c. Genetic algorithms to determine JONSWAP spectra parameters. Ocean Dyn. https://doi.org/10.1007/s10236-019-01341-8

Rueda-Bayona, J.G., Guzmán, A., Silva, R., 2020d. Genetic algorithms to determine JONSWAP spectra parameters. Ocean Dyn. https://doi.org/10.1007/s10236-019-01341-8

Rueda-Bayona, J.G., Horrillo-Caraballo, J., Chaparro, T.R., 2020e. Modelling of surface river plume using set-up and input data files of Delft-3D model. Data Br. https://doi.org/10.1016/j.dib.2020.105899

Rueda-Bayona, J.G., Osorio-Arias, A.F., Guzmán, A., Rivillas-Ospina, G., 2019b. Alternative method to determine extreme hydrodynamic forces with data limitations for offshore engineering. J. Waterw. Port, Coast. Ocean Eng. 145. https://doi.org/10.1061/(ASCE)WW.1943-5460.0000499

Sant, T., Buhagiar, D., Farrugia, R.N., 2018. Evaluating a new concept to integrate compressed air energy storage in spar-type floating offshore wind turbine structures. Ocean Eng. 166, 232–241. https://doi.org/10.1016/j.oceaneng.2018.08.017

Sarkar, S., Chen, L., Fitzgerald, B., Basu, B., 2020. Multi-resolution wavelet pitch controller for spar-type floating offshore wind turbines including wave-current interactions. J. Sound Vib. 470, 115170. https://doi.org/10.1016/j.jsv.2020.115170

Sarpkaya, T., 1993. Offshore Hydrodynamics. ASME J. Offshore Mech. Artic Eng. 115, 2–5. https://doi.org/10.1115/1.2920085

Tian, Y., Gaudin, C., Randolph, M.F., Cassidy, M.J., Peng, B., 2018. Numerical investigation of diving potential and optimization of offshore anchors. J. Geotech. Geoenvironmental Eng. 144, 1–9. https://doi.org/10.1061/(ASCE)GT.1943-5606.0001830

Yue, M., Liu, Q., Li, C., Ding, Q., Cheng, S., Zhu, H., 2020. Effects of heave plate on dynamic response of floating wind turbine Spar platform under the coupling effect of wind and wave. Ocean Eng. 201, 107103. https://doi.org/10.1016/j.oceaneng.2020.107103